RSC Advances

ROYAL SOCIETY OF CHEMISTRY

www.rsc.org/advances

Journal Name

RSCPublishing

COMMUNICATION

Mg-doped TiO_2 nanorods improving open-circuit voltages of ammonium lead halide perovskite solar cells

Cite this: DOI: 10.1039/x0xx00000x

K. Manseki,[a] T. Ikeya,[a] A. Tamura,[a] T. Ban,[a] T. Sugiura[a] and T. Yoshida[a, b, *]

Received 00th January 2012,
Accepted 00th January 2012

DOI: 10.1039/x0xx00000x

www.rsc.org/

Mg-doped TiO_2 nanorods were successfully synthesized from colloidal titanate by a microwave hydrothermal reaction. Use of such TiO_2 having an elevated conduction band edge as an electron extracting material for ammonium lead halide perovskite solar cells resulted in an increase of V_{oc} as much as 215 mV.

Solution processible solar cells currently attract widespread interest as a potential cost-effective technology for sustainable energy systems.[1] Among them, organo-lead halide perovskite cells provide intriguing performance, offering a remarkable light-to-electricity conversion efficiency of as high as 15% that fulfils a benchmark for practical applications.[2] However, several criteria, such as broad range photon harvesting from visible to near-infrared region, durability of devices, scaling up of devices and reproducibility of their performance, should be addressed in the up-coming stage of research. Besides these points, the choice of materials for carrier selective contacts can offer possibilities for optimizing open circuit voltage (V_{oc}).[3] Electron-selective contact has typically been titanium dioxide (TiO_2). A question arises for possible application of other oxides and also about the need of mesoporous nanostructure that has been essential for achieving high efficiencies in dye-sensitized solar cells (DSSCs).[4] Should we regard this system as a version of solid-state DSSC in which dye molecule is simply substituted by the perovskite compound, or should it be a version of p-i-n solar cell (same as flat junction device) that can be solution processed? We need a lot more elaborative work to answer this question.

Several groups have already demonstrated that V_{oc} can be tuned by hole-transporting material (HTM), such as spiro-OMeTAD and poly-triarylamine, although perovskite absorber itself seem to act as both electron and hole-transporter.[5] Up to around 1.2 V has been achieved so far.[6] Another possibility for the V_{oc} increase lies in the development of metal oxide layer that acts as the electron-selective contact and provide a pathway for electron transport. Tuning of the conduction band position by metal ion doping into the crystal lattice of oxide photoanode materials has been a successful strategy in DSSCs. Iwamoto et al. has reported a marked upward shift of the conduction band of TiO_2 by the substitution of Ti(IV) with Mg(II).[7] They also noted a V_{oc} increase up to around 1 V for organic dye based DSSCs employing iodine-iodide electrolytes. The reported nanoparticles are, however, prepared via a long time hydrothermal process at a high temperature of 300°C, which will hamper practical applications for use in low-cost solar cells.

This communication presents the rapid synthesis of Mg-doped single crystal TiO_2 nanorods possessing a relatively high conduction band potential as compared to undoped TiO_2 analogue with the same morphology, which can be obtained from colloidal titanate in a mild hydrothermal condition at 180°C and 1h. We have compared them as electron extracting contact materials in ammonium lead halide perovskite ($CH_3NH_3PbI_3$) cells employing poly-3-hexylthiophene (P3HT) as the HTM and found a marked increase of V_{oc} from 587 to 802 mV by Mg doping.

We recently reported a microwave-assisted hydrothermal synthesis of single crystal TiO_2 nanorods elongated along the *c*-axis of anatase.[8] Nanorods with 15 nm width and 40 nm length enabled a saturated adsorption of N719 dye molecules in a densely packed monolayer that achieved an incident photon to current conversion efficiency as high as 85.6 %.[9] Following the successful establishment of the rapid synthetic technique of high performance TiO_2, we have attempted Mg doping to the nanorod as shown in Fig. 1. It is of significant importance that both the rod-shape morphology and the size could be preserved with the Mg content of 5 % ([Mg(II)]/[Ti(IV)] = 0.05) as seen from the SEM and TEM images in Fig. 2, so that the observed difference in the photovoltaic performance can directly be attributed to the difference of their energetic structure. The controlled pH at around 8.1 allows size-tunable anisotropic crystal growth of the nanorods, in which the

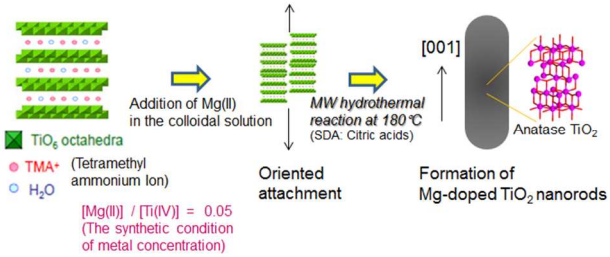

Fig. 1 Schematic drawing of the synthesis of Mg-doped TiO_2 nanorods using colloidal titanate as a starting material.

existence of Mg ion was confirmed by SEM-EDX measurement (Fig. S1 in Supporting information). HR-TEM images in Fig. 2 revealed lattice fringes with spacing of d = 0.35 nm corresponding to that in between anatase 101 planes. The lattice fringe spread over the entire nanoparticle without dislocations, proving its single crystalline structure. Essentially the same TEM images were obtained also for the Mg-doped material, indicating no deterioration of crystallinity by Mg doping. From the XRD patterns (Fig. S2), no biproduct phases of $MgTiO_3$ or $MgTi_2O_5$ was identified. Therefore, it is postulated that single phase Mg-doped TiO_2 crystals formed by the synthetic conditions we employed.

Fig. 3 shows UV-vis diffuse reflectance spectra of the annealed porous films consisting of TiO_2 nanorods with and without Mg doping. The absorption onset is clearly shifted towards the higher energy by Mg doping. The optical bandgaps estimated by Tauc plot ($[F(R_\infty)h\nu]^{1/2}$ vs. eV) indicated a bandgap increases from 3.29 eV to 3.38 eV. The incorporation of Mg into TiO_2 nanorod motif produced Mg(II)-substituted crystal lattice in anatase TiO_2, allowing TiO_2 nanocrystals to possess higher-lying conduction band. It is worth noting that TiO_2 electronic structures can be manipulated via a relatively mild hydrothermal reaction from colloidal titanate, although it cannot be ruled out that an amorphous thin layer of MgO or Mg hydroxides forms on the surface of TiO_2, which, however, cannot contribute to the observed bandgap increase.

In order to visualize the interface structures involving the edges of TiO_2 crystals and light-absorbing $CH_3NH_3PbI_3$, HR-TEM image was also obtained for a sample after spin-coating the perovskite onto the annealed Mg-doped TiO_2 nanorod films. As shown in Fig. 2(d), spherical dots of around 2~3 nm in size were observed on the surface of randomly oriented titania nanorods. The UV-vis absorption spectrum of the same sample (Fig. S3) covers an entire region of the visible light. This means that the $CH_3NH_3PbI_3$ can capture much of incident photons for charge separation, in spite of that still much of the surface of the TiO_2 nanorods remain uncovered. When P3HT is successively deposited, it should find a contact not only with the perovskite but also with the bare surface of TiO_2.

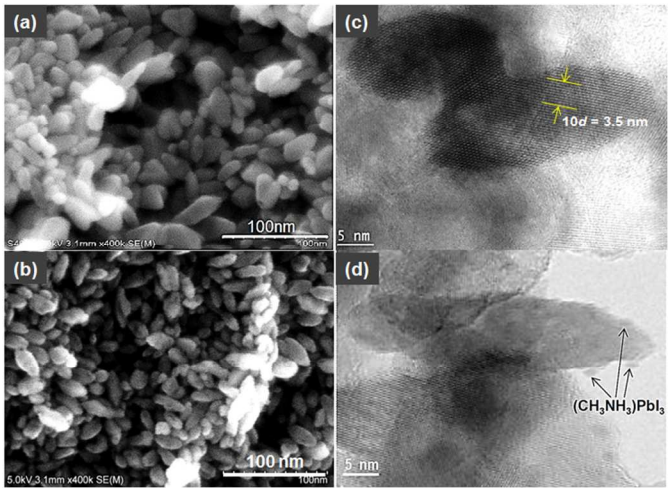

Fig. 2 SEM images of TiO_2 nanorods (a) and Mg-doped TiO_2 nanorods (b) prepared via a microwave hydrothermal reaction. HR-TEM images of the films obtained by sintering non-doped TiO_2 nanorods (c) and Mg-doped TiO_2 nanorods to which $CH_3NH_3PbI_3$ perovskite was deposited by spin coating (d). The arrows in (d) indicate the existence of $CH_3NH_3PbI_3$ dots.

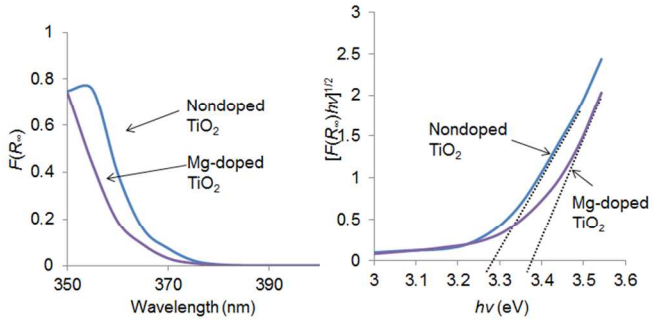

Fig. 3 UV-Vis diffuse reflectance spectra of TiO_2 nanorods with and without Mg doping.

After completing devices by depositing Au contact, the cell properties were compared. As shown in Table 1 and Fig. 4, a prominent improvement of photovoltaic performance was observed for Mg-doped TiO_2 nanorods. Although the short circuit photocurrent (J_{sc}) slightly decreased, the V_{oc} dramatically increased as much as 215 mV and the fill factor (*FF*) was also clearly improved with the Mg-doped TiO_2 nanorods. As a consequence, the overall energy conversion efficiency was increased from 3.14 to 4.17% simply by changing the material for electron extraction. We have also employed these two kinds of porous TiO_2 with similar thickness (ca. 4 μm) as photoelectrodes for DSSCs employing N719 as the sensitizer (Table 1). Not as prominent as that in the solid devices, but the Mg doping lead to a clear enhancement of V_{oc} from 770 to 833 mV.

The alignment of the energy levels of the present devices can be drawn as Fig. 4(c). The band position of anatase TiO_2 is taken from literature.[5] Mg doping lead to an increase of bandgap for about 0.1 eV. Assuming a symmetrical broadening of the bandgap, the position of the conduction band edge of the Mg-doped TiO_2 should be located at around -3.95 eV (vs. VAC). Conduction band edge of organo-lead halide perovskite consisting of methylammonium iodide is supposed to lie around -3.9 eV, according to the literature.[9] The slight decrease of J_{sc} for the perovskite cells by Mg doping can be attributed to the minimal difference of the conduction band positions to decrease the efficiency of electron transfer. Such a decrease was indeed not observed for the DSSCs sensitized with N719 dye as its LUMO level (-3.76 eV[10]) is well above the conduction band edge of both types of TiO_2.

On the other hand, the increase of V_{oc} for the perovskite cell is far beyond that expected from the elevation of the conduction band edge by Mg doping, while that for the DSSCs almost coincides with the shift of the conduction band. Suppressed recombination by the possible presence of Mg oxide, hydroxide species on the surface of Mg-doped TiO_2 nanorod can be the additional reason for the remarkable increase of V_{oc}.[11] The dark current of the Mg-doped device is significantly reduced as compared to the non-doped device, indicating small leakage current to increase the electron concentration under illumination to achieve a high V_{oc}. Recently, Snaith et al. has also reported an increase of V_{oc} (from 0.68 to 0.81 V) by insertion of fullerene monolayer in between TiO_2 and P3HT in their high-performance perovskite-polymer hybrid cells.[9] Since much of the bare TiO_2 surface should be in contact with P3HT as indicated from the HR-TEM observation, passivation of the TiO_2 surface should be effective to increase V_{oc}.

It should also be noted that the results of the present study support the idea of mesoporous TiO_2 "sensitization" by nano-sized dots of the perovskite compound as depicted in Fig. 4, rather than solution processible p-i-n flat junction, since relatively thick (4 μm) porous TiO_2 only partly covered with the perovskite compound, thus allowing direct contact to P3HT, could work rather nicely.

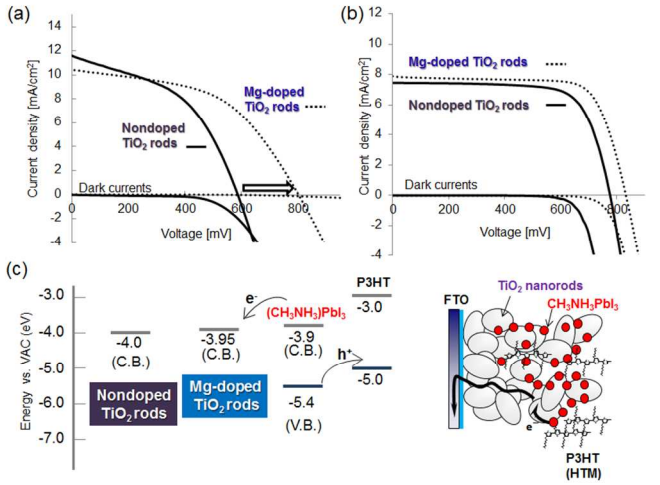

Fig. 4 *I-V* curves of the $CH_3NH_3PbI_3$ perovskite cells (a) and N719 sensitized cells (b) employing undoped and Mg-doped TiO_2 nanorods in the dark and under illumination with AM 1.5 simulated sun light (100 mW cm^{-2}). The energy band diagram of these cells (c).

Table 1 Photovoltaic performance of the $CH_3NH_3PbI_3$ perovskite cells and N719 sensitized cells employing undoped and Mg-doped TiO_2 nanorods. TiO_2 layer thickness was adjusted to ca. 4 μm.

TiO_2	Absorbers	J_{sc}(mA/cm²)	V_{oc}(mV)	*FF*	η(%)
Mg-doped TiO_2	$CH_3NH_3PbI_3$	10.4	802	0.50	4.17
Nondoped TiO_2	$CH_3NH_3PbI_3$	11.6	587	0.46	3.14
Mg-doped TiO_2	N719	7.90	833	0.74	4.90
Nondoped TiO_2	N719	7.50	777	0.72	4.20

Conclusions

The method of microwave-assisted hydrothermal rapid crystallization of nanorod TiO_2 from layered titanate precursor was successfully applied to the synthesis of Mg-doped TiO_2 nanorod having a broadened bandgap but the same size and shape. These materials were employed as electron extracting and transporting layers for the $CH_3NH_3PbI_3$ perovskite cells and N719 sensitized cells to prove the usefulness of Mg doping to gain high V_{oc}s. The significant V_{oc} increase (215 mV) in case of the perovskite cell cannot solely be attributed to the elevated conduction band edge but to the suppressed recombination at the Mg-doped TiO_2 / P3HT interface due to the possible presence of Mg oxide / hydroxide layer on the surface of the nanorod. However, the present study has clearly demonstrated possibilities of voltage optimization by controlling the energetic structure of the electron extracting material to be combined with the ammonium lead halide perovskite absorber for which bandgap tuning is also possible, for example, by changing the blend of halide anions.[12] Such energy level tuning including the use of alternative HTM else than P3HT should be one of the most reasonable strategy to push up the efficiency.

This work is supported by the Japan Society for the Promotion of Science (JSPS) through its ''Funding Program for World-Leading Innovative RD on Science and Technology (FIRST Program).''

Notes and references

[a]*Environmental and Renewable Energy Systems (ERES) Division, Graduate School of Engineering, Gifu University, Yanagido 1-1, Gifu 501-1193, Japan*

[b]*Department of Chemistry and Chemical Engineering, Faculty of Engineering, Yamagata University, 4-3-16 Jonan, Yonezawa, Yamagata 992-8510, Japan.* E-mail: yoshidat@yz.yamagata-u.ac.jp

†

Electronic Supplementary Information (ESI) available: [details of any supplementary information available should be included here]. See DOI: 10.1039/c000000x/

1 Recent examples: M. Grätzel, Rene. A.-J. Janssen, D.-B. Mitzi and E.-H. Sargent, *Nature*, 2012, **488**, 304; M.-M. Lee, J. Teuscher, T. Miyasaka, T.-N. Murakami and H.-J. Snaith, *Science*, 2012, **338**, 643.

2 J. Burschka, Ntzel. Pellet, S.-J. Moon, R.-H. Baker, P. Gao, M.-K. Nazeeruddin and M. Grätzel, *Nature*, 2013, **499**, 316; M. Liu, M.-B. Johnston and H. J. Snaith, *Nature*, 2013, **501**, 395; S.-D. Stranks, G.-E. Eperon, G. Grancini, C. Menelaou, M.-J. P. Alcocer, T. Leijtens, L.-M. Herz, A. Petrozza and H. J. Snaith, *Science*, 2013, **342**, 341; G. Xing, N. Mathews, S. Sun, S.-S. Lim, Y.-M. Lam, M. Grätzel, S. Mhaisalkar and T.-C. Sum, *Science*, 2013, **342**, 344.

3 H.-J. Snaith, *J. Phys. Chem. Lett*, 2013, **4**, 3623; D. Bi, S.-J. Moon, L. Haggman, G. Boschloo, L. Yang, Eric. M.-J. Johansson, M.-K. Nazeeruddin, M. Grätzel and A. Hagfeldt, *RSC Adv.*, 2013, **3**, 18762.

4 Recent examples: A. Hagfeldt, G. Boschloo, L. C. Sun, L. Kloo and H. Pettersson, *Chem. Rev.,* 2010, ***110***, 6595; M. Grätzel, *Acc. Chem. Res.*, 2009, **42**, 1788; J. Yan and F. Zhou, *J. Mater. Chem.*, 2011, **21**, 9406.

5 J.-H. Heo, S.-H. Im, J.-H. Noh, T.-N. Mandal, C.-S. Lim, J.-A.Chang, Y.-H. Lee, H.-J. Kim, A. Sarkar, M.-K. Nazeeruddin, M. Grätzel and S. II Seok, *Nat. Photonics*, 2013, **7**, 487; J. Qiu, Y. Qiu, K. Yan, M. Zhong, C. Mu, H. Yan and S. Yang., *Nanoscale*, 2013, **5**, 3245; N.-G. Park, *J. Phys. Chem. Lett*, 2013, **4**, 2423; P.-V. Kamat, *J. Phys. Chem. Lett*, 2013, **4**, 3733.

6 B. Cai, Y. Xing, Z. Yang, W.-H. Zhang and J. Qiu, *Energy Environ. Sci*., 2013, **6**, 1480.

7 S. Iwamoto, Y. Sazanami, M. Inoue, T. Inoue, T. Hoshi, K. Shigaki, M. Kaneko, A. Maenosono, *ChemSusChem.*, 2008, **1**, 401.

8 K. Manseki, Y. Kondo, T. Ban, T. Sugiura and T. Yoshida, *Dalton Trans.*, 2013, **42**, 3295.

9 A. Abrusci, S.-D. Stranks, P. Docampo, H.-L Yip, A. K.-Y. Jen, H.-J. Snaith, *Nano Lett.*, 2013, **13**, 3124.

10 F. De Angelis, S. Fantacci, E. Mosconi, M.K. Nazeeruddin and M. Grätzel, *J. Phys. Chem. C*, 2011, **115**, 8825.

11 J.-H. Yum, S. Nakade, D.-Y. Kim, S. Yanagida, *J. Phys. Chem. B*, 2006, **110**, 3215.

12 J.-H. Noh, S.-H. Im, J.-H. Heo, T.N. Mandal and S.-I. Seok, *Nano Lett.*, 2013, **13**, 1764.